

Article

MiR-337-3p Promotes Adipocyte Browning by Inhibiting TWIST1

Indira G. C. Vonhögen ¹, Hamid el Azzouzi ^{1,2}, Servé Olieslagers ¹, Aliaksei Vasilevich ³, Jan de Boer ³, Francisco J. Tinahones ^{4,5,6}, Paula A. da Costa Martins ^{1,7}, Leon J. de Windt ^{1,*} 
and Mora Murri ^{4,5} 

¹ Department of Molecular Genetics, Faculty of Sciences and Engineering, CARIM School for Cardiovascular Diseases, Faculty of Health, Medicine and Life Sciences, Maastricht University, 6200 MD Maastricht, The Netherlands; indira.vonhogen@maastrichtuniversity.nl (I.G.C.V.); h.elazzouzi@erasmusmc.nl (H.e.A.); s.olieslagers@maastrichtuniversity.nl (S.O.); p.dacostamartins@maastrichtuniversity.nl (P.A.d.C.M.)

² Department of Molecular Genetics, Erasmus University MC, 3015 GD Rotterdam, The Netherlands

³ BioInterface Science Group, Department of Biomedical Engineering and Institute for Complex Molecular Systems, Eindhoven University of Technology, 5600 MB Eindhoven, The Netherlands; a.vasilevich@tue.nl (A.V.); j.d.boer@tue.nl (J.d.B.)

⁴ Unidad de Gestión Clínica de Endocrinología y Nutrición, Instituto de Investigación Biomédica de Málaga (IBIMA), Hospital Clínico Virgen de la Victoria, 29010 Málaga, Spain; fjtinahones@hotmail.com (F.J.T.); moramurri@gmail.com (M.M.)

⁵ Centro de Investigación Biomédica en Red de Fisiopatología de la Obesidad y la Nutrición, CIBEROBn, Instituto de Salud Carlos III, 28029 Madrid, Spain

⁶ Faculty of Medicine, University of Malaga, 29010 Malaga, Spain

⁷ Department of Physiology and Cardiothoracic Surgery, Faculty of Medicine, University of Porto, 4200-319 Porto, Portugal

* Correspondence: l.dewindt@maastrichtuniversity.nl

Received: 28 March 2020; Accepted: 15 April 2020; Published: 23 April 2020



Abstract: The prevalence of metabolic syndrome (MetS) and obesity is an alarming health issue worldwide. Obesity is characterized by an excessive accumulation of white adipose tissue (WAT), and it is associated with diminished brown adipose tissue (BAT) activity. Twist1 acts as a negative feedback regulator of BAT metabolism. Therefore, targeting Twist1 could become a strategy for obesity and metabolic disease. Here, we have identified miR-337-3p as an upstream regulator of Twist1. Increased miR-337-3p expression paralleled decreased expression of TWIST1 in BAT compared to WAT. Overexpression of miR-337-3p in brown pre-adipocytes provoked a reduction in Twist1 expression that was accompanied by increased expression of brown/mitochondrial markers. Luciferase assays confirmed an interaction between the miR-337 seed sequence and *Twist1* 3'UTR. The inverse relationship between the expression of *TWIST1* and miR-337 was finally validated in adipose tissue samples from non-MetS and MetS subjects that demonstrated a dysregulation of the miR-337-Twist1 molecular axis in MetS. The present study demonstrates that adipocyte miR-337-3p suppresses Twist1 repression and enhances the browning of adipocytes.

Keywords: brown adipose tissue; microRNA; mitochondria; obesity; metabolic syndrome

1. Introduction

The worldwide prevalence of obesity has nearly tripled since 1975; more than 2.1 billion people are affected by obesity and overweight. It is a major health problem as it is associated with an increased risk of morbidity and mortality in the world, causing 3.4 million deaths and 3.9% of years of life lost

worldwide [1]. Overall, obesity is an insidious condition that is often complicated by the co-occurrence of hyperglycaemia, dyslipidaemia, and hypertension, which are classified together as the metabolic syndrome (MetS) [2]. Therefore, obesity requires effective therapeutic interventions. A proportion of obese individuals are protected against worsening of metabolic health, whereas, at the other end of the spectrum, there are normal weight individuals who have metabolic abnormalities usually associated with obesity, suggesting that adipose tissue physiology, rather than the amount of fat mass, may be a key factor in the pathophysiology of obesity-related metabolic disorders [3,4].

In recent years, adipose tissue has been recognized as a major endocrine organ, which plays a key role in energy homeostasis. In mammals, two types of adipose tissue can be distinguished from a histological and functional perspective: white (WAT) and brown adipose tissue (BAT) [5]. WAT is mainly involved in lipid storage within lipid droplets in the fed state, and release of fatty acids from the breakdown of stored triglycerides in the fasted state, whereas BAT utilizes neutral lipids stored in lipid droplets for the generation of heat and to meet cellular energetic requirements [5,6]. Morphologically, WAT adipocytes contain a single lipid droplet, and few mitochondria, while BAT adipocytes contain a high number of mitochondria and multiple small lipid droplets. In the last few years, beige adipocytes have been reported in WAT, which are brown-like adipocytes that contain medium mitochondria density and a few to many lipid droplets, and also have thermogenic capacity [7]. Obesity is associated with lower brown/beige adipocyte activity. A recent study has shown that obesity led to the development of a hypoxic state in BAT, diminished β -adrenergic signaling, mitochondrial dysfunction and loss, causing obesity-associated BAT whitening [8].

The essential role of mitochondria in numerous aspects of metabolic regulation, including energy supply, regulation of apoptosis, calcium homeostasis, and production of reactive oxygen species, position them at the center of the control of global energy homeostasis [9,10]. Mitochondrial metabolism is both the origin and target of multiple nutrient signals that orchestrate integrated physiological responses to maintain cellular insulin-sensitivity. To perform their key roles in cellular energy production, mitochondria use an intricate system that encompasses the breakdown of fatty acids and glucose, which is coupled to oxidative phosphorylation, generating cellular energy in the form of adenosine triphosphate (ATP). This central position of mitochondria makes them vulnerable to damage [11]. A metabolic imbalance of nutrient supply, energy production, and/or oxidative respiration results in “mitochondrial dysfunction”.

MicroRNAs (miRs) are functional non-coding RNAs that regulate gene expression at the post-transcriptional level. They play an important regulatory role in a variety of biological processes, including regulators of differentiation, development, and function of brown and beige adipocytes. Recently, several studies have identified several miRs involved in the regulation of browning [12,13]. In terms of therapeutic potential, miRs represent a novel and an attractive target to manipulate malignant body functions as their activity can be efficiently modulated with RNA-based antisense technology [14,15]. A transcriptional regulator, *Twist1*, has been reported to be mainly present in the adipose tissue and acts as a negative regulator of brown fat metabolism [16]. An *in vivo* study showed that transgenic mice expressing *twist-1* in the adipose tissue are susceptible to high-fat diet-induced obesity, whereas *twist-1* heterozygous knockout mice showed obesity-resistance [16]. Therefore, targeting *Twist1* by miRNA intervention could become a strategy for the treatment of obesity and metabolic disease.

The aim of the present study was to identify a miR that targets *Twist1* to modulate browning of adipocytes. A bioinformatic screen resulted in the identification of potential miRs capable of repressing *Twist1* in adipocytes, promoting browning by counteracting the inhibition of brown fat metabolism and mitochondrial biogenesis. As a validation of this screen, miR-337-3p was found to be most enriched in BAT. Overexpression of miR-337-3p enhanced brown fat metabolism by a reduction in *Twist1* and an increased expression of the downstream uncoupling protein 1 (UCP1) thermoregulatory effector protein. The proposed relationship was further substantiated by validation of seed complementarity, confirming the interaction between miR-337-3p and *Twist1* 3'UTR. Altogether, our results show that miR-337-3p

plays a role in the modulation of browning of adipocytes by targeting Twist1. The concordance of the proposed mechanism and validation in human samples has raised interesting grounds for corroborating its therapeutic potential in counteracting obesity and metabolic syndrome.

2. Materials and Methods

2.1. Screening of Brown Inducing miR Candidates

Genes repressing browning of adipose tissue were selected based on a literature screen performed in PUBMED (Table S2). miR candidates were identified by imputing selected genes identified through literature in miR target prediction tools, miR-Base (<http://www.mirbase.org/>; The University of Manchester, Manchester, UK) and miRNAviewer (<http://cbio.mskcc.org/mirnaviewer/>; Memorial Sloan-Kettering Cancer Center, New York, NY USA) (Table S2). Candidates were further screened, analysing the endogenous expression in mouse brown and white adipose tissue by quantitative real-time PCR. Following the screen, the miRNA candidate that was most enriched in mouse BAT compared to WAT was further validated by in vitro functional analysis for its browning ability. Throughout our manuscript, we adhered to the animal research: reporting of in vivo experiments (ARRIVE) guidelines (<https://www.nc3rs.org.uk/arrive-guidelines>) for reporting the in vivo animal studies.

2.2. Quantitative RT-PCR

Total RNA was extracted from mouse and human tissue and mouse-derived cultured cell lines using TRIzol reagent from the Direct-Zol™ RNA Miniprep kit (R2051) following the manufacturer's protocol. Total RNA was reversely transcribed using a miScript II RT Kit (218161 Qiagen, Hilden, Germany), while mRNA templates were reversely transcribed using the Moloney Murine Leukemia Virus (M-MLV RT) reverse transcriptase by Promega (9PIM170; Promega, Madison, WI, USA). RT-PCR was performed using SYBR green, carried out on a Bio-Rad CFX96 Real-Time System. For validation of transfection efficiency in cell culture experiments, miR-337-3p pre-designed miRCURY LNA Uni RT primer mix (339306, Qiagen) was used. Consequently, total RNA was reversely transcribed using its compatible miRCURY LNA™ Universal cDNA synthesis kit II (203301, Qiagen) followed by real-time PCR with the LNA enhanced primers using ExiLent SYBR green (203401, ThermoFisher, Waltham, MA, USA). Quantification of transcript level by RT-PCR was done by using the relative Ct ($\Delta\Delta Ct$) method. mRNA transcripts were normalized to *L7*, while miR transcripts were normalized to *U6* or *5s* (pre-designed miRCURY LNA Uni RT primer mix, Qiagen). The choice of reference genes was based on their stability in the different samples analyzed. The sequence of the primers used in this study can be found in Table 1.

2.3. Western Blot Analysis

Whole cell and tissue lysates were homogenized in protein lysis buffer (IGEPAL 1%, SDS 0.5%, NaCl 150 mM, Tris-HCl 50 mM pH 8.5, EDTA 5 mM) supplemented by a protease inhibitor cocktail and PhosSTOP complete (Roche Applied Sciences, Penzberg, Bavaria, Germany). Supernatants from cell lysates were briefly centrifuged, while tissue lysates were centrifuged successively (12,000× *g*, 4 °C, 20 min) followed by protein quantification by the BCA Protein Assay Kit (Thermo Scientific, Rockford, IL, USA). Samples supplemented by 4× Laemmli buffer and 5% β-mercaptoethanol were boiled at 42 °C for 25 min, separated by 10% and 12% SDS-polyacrylamide gel and transferred to nitrocellulose blotting membrane (Amersham™ Protran™ 0.45 μM NC, GE Healthcare LifeScience, Chicago, IL, USA). Blotted membranes from tissue samples were stained for total protein detection using the Li-COR REVERT Kit following the manufacturer's instructions (Li-Cor Biosciences GmbH, Bad Homburg vor der Höhe, Germany). Total protein stain (TPS) was then removed by reversal solution LI-COR 0.1M sodium Hydroxide, 30% methanol in water. Next, membranes were blocked for 1 h at room temperature in Odyssey PBS blocking buffer (LI-COR 927-40100), and each membrane was incubated with primary antibodies in Odyssey PBS blocking buffer 0.1% Tween) overnight at 4 °C. Next,

membranes were washed 3× (PBS-T), incubated at room temperature for 1 h with secondary antibodies, washed 3× PBS-T, and imaged (multiplexed analysis) on an Odyssey Clx imaging system (LI-COR) at an automatic scanning resolution of 169 µm and automatic image quality setting. Images were analyzed by quantification of band densitometry by ImageJ. For single target detection, membranes were blocked with 10% milk in TBS-T, all washing and incubations were performed in TBS-T 5% milk and incubations with secondary antibodies followed by image detection. Furthermore, images for single target detection were generated using Extreme Sensitivity Chemiluminescence Substrate (NEL 112001EA) on a 3000 image Analyzer (Fujifilm). Primary antibodies included anti-TWIST1 (T6451 Sigma affinity isolated produced in rabbit 1:500; Sigma-Aldrich, Saint Louis, MO, USA); OXPHOS rodent antibody cocktail (Abcam 110413 1:1000, Abcam, Cambridge, UK); anti-UCP1 (U6382 Sigma produced in rabbit 1:1000); anti-ACTB (A1978 Sigma monoclonal produced in mice 1:1000) as the loading control for cell lysates and anti-GAPDH (1:1000) Mouse Monoclonal (Millipore MAB374, Merck-Millipore, Burlington, MA, USA) as the loading control for tissue lysates. Secondary antibodies included IRDye 800CW Goat anti-Mouse IgG (LI-COR 926 32210) and IRDye 680RD Donkey anti-Rabbit (LI-COR 925 68073) at 1:10000 for multiple target detection, and polyclonal rabbit anti-mouse IgG-HRP (DAKO 1:2000, Agilent Technologies, Santa Clara, CA, USA) and polyclonal swine anti-rabbit IgG-HRP (DAKO 1:2000, Agilent Technologies) for single target detection. Results are presented in densitometry arbitrary units as an n-fold increase over ACTB for cells, GAPDH, or TPS for tissue samples.

Table 1. Primer sequences.

Gene Name	Gene ID	Sequence	
Primers for <i>Mus Musculus</i>			
<i>L7</i>	NM_011291	Forward	GAAGCTCATCTATGAGAAGGC
		Reverse	AAGACGAAGGAGCTGCAGAAC
<i>Twist1</i>	NM_011658	Forward	CAGGCCGGAGACCTAGATG
		Reverse	CCACGCCCTGATTCTTGTG
<i>Cs</i>	NM_026444	Forward	TAAGGAGCAGGCCAGAATTAAG
		Reverse	CCGAAGTCTCATAACAAGTCC
<i>Crls1</i>	NM_001024385	Forward	GCTCTTGATCCACTTGCTGATA
		Reverse	GTAAGTGAGTGGGACTGGAATAAG
<i>Ucp1</i>	NM_009463	Forward	GGGAGAGAAACACCTGCCTCT
		Reverse	GGGAGAGAAACACCTGCCTCT
<i>Cox8b</i>	NM_007751	Forward	TTGGGGCCAAGGAAGGAGTG
		Reverse	GAGATCCCCACAGCCTGCTC
miR-337-3p			TCAGCTCCTATATGATGCCTTT
Primers for Humans			
<i>TWIST1</i>	NM_000474	Forward	GCTCAGCTACGCCTTCTC
		Reverse	TGTCATTTTCTCCTTCTCTGG
<i>CS</i>	NM_004077	Forward	GGCCATTGACTCTAACCTGG
		Reverse	CACTTACATTGCCACCTCA
<i>CRLS1</i>	NM_019095	Forward	ATGACGAGAATTGGCTTGGC
		Reverse	TTGATTGGCCAGTTTCGA
<i>UCP1</i>	NM_021833	Forward	CGGAATCAAACCTCGCTACA
		Reverse	TGACACTTCTCATCAGATTGGG
<i>TCF21</i>	NM_003206	Forward	CAGATCCTGGCTAACGACAA
		Reverse	CGGTCACTACTTCTTCAGG

2.4. Cell Culture

Immortalized brown pre-adipocytes were obtained from Dr. Bruce Spiegelman, Harvard Medical Center, and maintained in DMEM (1×)-Glutamax (Gibco) with 20% FBS and 100 µg/mL Pen/Strep (Gibco-BRL, Life Technologies Ltd., Paisly, UK) in a humidified atmosphere of 5% CO₂ at 37 °C [17].

Immortalized brown pre-adipocytes were reversely transfected with 10 nM of precursor or 100 nM of miRCURY LNA inhibitor specific for mmu-miR-337-3p or precursor scrambled miR or LNA inhibitor negative control, respectively, with 4 µL of Oligofectamin (Invitrogen, Life Technologies, Carlsbad, CA, USA) per well of a 6-wells plate following the manufacturer's protocol. Transfected pre-adipocytes were grown to confluence (day 0) and induced to differentiation as previously described [17].

2.5. Luciferase Assay

Constructs bearing 713 base pairs of murine *Twist1* 3' untranslated region (UTR) were sub-cloned in pmiRGLo Dual-Luciferase miR Target expression Vector (Promega, Madison, WI, USA). COS7 cells maintained in DMEM, with 10% FBS, 100 µg/mL Penicillin/Streptomycin, 10 µg/mL gentamycin, 100 µg/mL L-glutamine, and seeded in 48-well plates (24,000 cells/well) were transfected with the reporter plasmid containing *Twist-1* 3' untranslated region (UTR) using X-tremeGene 9 DNA transfection reagent followed by co-transfection with mmu-miR-337-3p precursor or LNA inhibitor or precursor scrambled miR negative control or LNA inhibitor negative control using oligofectamin transfection reagent (Invitrogen), as previously described. After 48 h, the luciferase activity was quantified using a Dual-Glo luciferase assay system (Promega) on a Luminometer. Firefly luciferase activity was normalized to renilla luciferase activity as an internal control.

2.6. Immunofluorescence and Detection of Mitochondrial Activity

Immortalized brown pre-adipocytes were grown to confluence (day 0) and induced to differentiation as previously described [17]. At day 0 and day 5 of differentiation, cells were washed twice with PBS and fixed with 4% paraformaldehyde. Mitochondrial staining of day 0 and day 5 cells was performed by mouse monoclonal Anti-ATPB Antibody (Abcam ab14730 1:500, Abcam) with overnight incubation at room temperature, washed 2 times with PBS followed by Secondary Goat anti-Mouse IgG H&L (Abcam ab150119 1:5000, Abcam) and HSC LipidTOX™ Green neutral lipid stain (Invitrogen H34475 1:1000, Life Technologies) for lipid droplet staining, then incubated for 1 h at room temperature. Subsequently, cells were washed 2 times with PBS and stained with DAPI (Sigma D9542 1:2000, Sigma-Aldrich) and imaged with a Nikon (Tokyo, Japan) Eclipse Ti_E epi-fluorescent inverted microscope. The sample was excited with an LED Spectra4 light source either with 390, 475, 549, or 632 nm. The emitted light, with wavelength 430, 488, 561, or 647 nm, correspondingly, were recorded with an Andor Zyla 5.5 4MP Mono camera. Number, integrated staining intensity, and area of mitochondria and lipid droplets were quantified from day 0 and day 5 cells and corrected for the total number of cells per image and displayed as median ± SD.

2.7. Mouse Adipose Tissue Isolation

Mouse WAT was isolated from inguinal subcutaneous adipose fat depots, while BAT was isolated from the interscapular brown adipose fat depot, from wild type adult mouse in a BL6BAF1 background (n = 8). After extraction of fat depots, the tissue was immediately frozen by immersion in liquid nitrogen and stored at −80 °C for subsequent RNA and protein extraction. Identity of BAT and WAT was confirmed by RNA expression of BAT specific markers. The mice used in the study were housed in climate-controlled, 12 h light–dark cycle with ad libitum access to chow diet and water. Experimental procedures involving animals were reviewed and approved by the Animal Facility of Maastricht University (DEC2014-076 on the 13th of May 2016).

2.8. Human Sample Collection

Subcutaneous and visceral adipose tissue (SAT and VAT) was obtained from MetS subjects submitted to bariatric surgery or non-MetS subjects submitted to laparoscopic surgery due to hiatal hernia or cholelithiasis [18]. The patients completed a structured interview to obtain the following data: sex, age, medical history, and drug consumption. All subjects underwent a standardized anthropometric examination: weight, height, blood pressure, waist and hip circumferences, and biochemical parameters

(Supplementary Table S1). None of the subjects were receiving orally administered antidiabetic agents or insulin therapy. Exclusion criteria included severe cardiac disease with prohibitive anaesthetic risks, major cardiovascular disease within 6 months prior to study inclusion, evidence of acute or chronic inflammatory disease, severe coagulopathy, tobacco and alcohol abuse, or inability to comply with nutritional requirements, including life-long vitamin replacement. All participants gave their informed consent, and the study was reviewed and approved on the 28th of December of 2015 by the ethics and research committee of Virgen de la Victoria Clinical University Hospital (Malaga, Spain).

2.9. Statistics

All results are displayed by means and standard error of means (SEM). Statistical analyses were performed in Prism (GraphPad Software, San Diego, CA, USA) and SPSS IBM 24 (IBM, Armonk, NY, USA). Normality of the distribution of continuous variables was assessed using the Shapiro–Wilk test. Logarithmic transformations ensured normal distribution of variables as needed. The relation between mouse WAT versus BAT; mouse BAT cells at day 0 vs day 5, BAT cells with precursor scramble vs. pre-miR-337-3p; BAT cells with LNA scramble vs. LNA-miR-337-3p; human non-MetS vs. MetS; were evaluated by either Mann–Whitney-U test for independent samples containing non-normal distributions or independent sample *t*-test for normal distribution data. For dependent samples, comparison between human SAT versus VAT, a Wilcoxon rank sum test was applied for non-normal distributions and Paired sample *t*-test for normal distributions. Spearman rank correlation analyses were performed for non-normal distributed data to analyze the correlation between miR expression levels from human adipose tissue and anthropometric and biochemical parameters. Significance level was set at $p < 0.05$. The heatmap was generated using Cluster 3.0, Mac OS X v10.0 (Stanford University, San Francisco, CA, USA) and Treeview software, V2.0.8 (Softonic International, Barcelona, Spain).

3. Results

3.1. miR-337 is a Potential Regulator of Browning of Adipose Tissue

The expression of Let-7c, miR-199a-5p, miR-151-3p, miR-145-5p, Let-7b-3p, miR-24-3p, miR-361-5p, miR-337-3p, miR-134-5p were assessed in murine BAT and WAT. Among these candidate miRs, miR-337-3p showed the largest fold change with an increased expression in BAT compared to WAT. (Figure 1a–d) The brown expression marker and mitochondrial marker *Ucp1*, cardioplipin synthase (*Crls1*), and citrate synthase (*Cs*), respectively, confirmed BAT phenotype from adipose tissue isolated from the intrascapular region from mice (Figure 1b). miR-337-3p is an intergenic non-coding RNA located on chromosome 14 of the human genome overlapping with the Al 117190.1 long non-coding RNA, for which no particular function or interaction with miR-337-3p has been reported. Besides this, miR-337-3p is conserved among species indicating resistance to evolutionary pressure (Figure 1e). RT-PCR analysis revealed that although miR-337-3p was expressed in murine skeletal muscle, brain, and WAT with very low expression levels in liver, kidney, small intestine, and pancreas, it was most enriched in BAT (Figure 1d). In comparison to WAT, there is a 7-fold increase in the expression of miR-337-3p in BAT (Figure 1c).

3.2. miR-337 Is Upregulated During Browning

Next, we analysed miR-337-3p expression during the differentiation of murine brown pre-adipocytes (day 0) towards mature brown adipocytes (day 5). Successful differentiation of brown adipocytes was confirmed by an increased expression of *Ucp1*, cytochrome C oxidase subunit 8b (*Cox8b*), and *Cs*, whereas *Crls1* showed the same trend (Figure 2c). Phenotypical characterization by immunofluorescence showed an increase in both mitochondria (ATPB) and lipid droplets (Lipidtox™) from day 0 to day 5 of differentiation (Figure 2a,b). Western blot analysis confirmed an increased protein abundance of several complexes of OXPHOS, suggesting increased mitochondrial respiration from day 0 to day 5 of differentiation of brown adipocytes (Figure 2d). Ultimately, alongside these

prominent changes occurring during the maturation of murine brown adipocytes, there is a 7-fold increased expression of miR-337-3p from day 0 to day 5 of differentiation (Figure 2e). Taken together, these findings indicate a potential role for miR-337-3p as a regulator of browning of adipose tissue and a possible modulator of mitochondrial function.

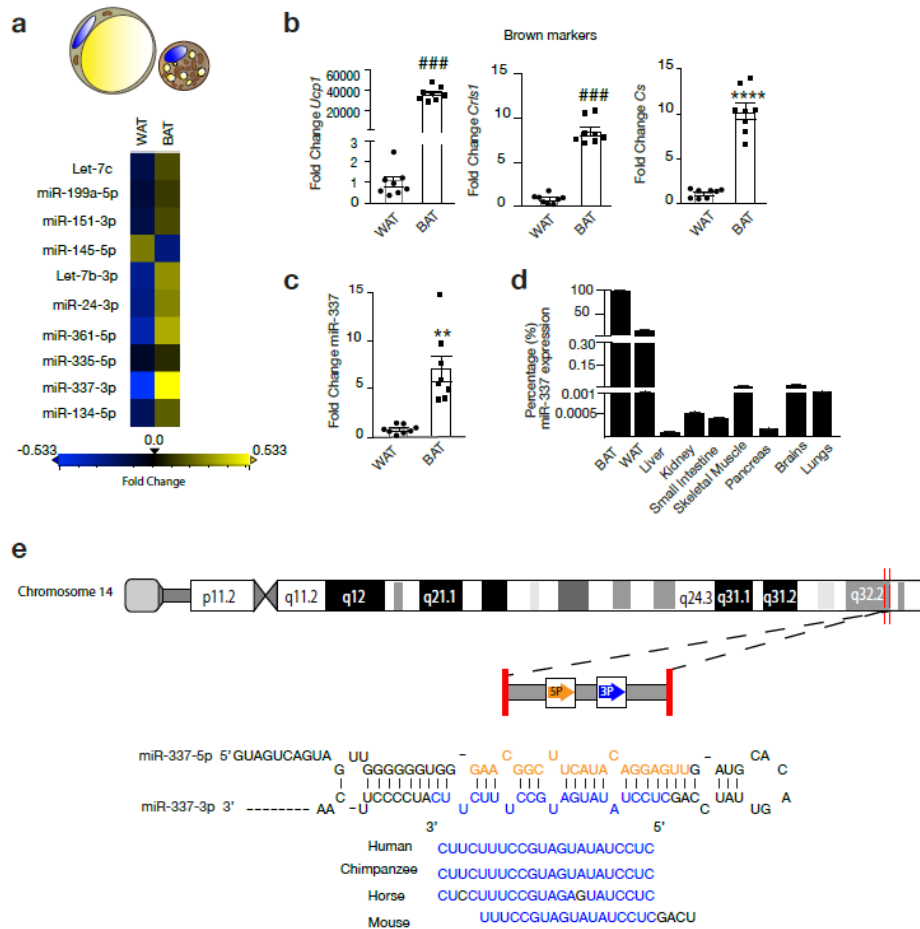


Figure 1. miR-337-3p is a potential regulator of browning of adipose tissue. **(a)** Representative heatmap showing the results of RT-PCR analysis used to screen a panel of microRNAs (miR) in mouse white adipose tissue (WAT) and brown adipose tissue (BAT): Let-7c, miR-199a-5p, miR-151-3p, miR-145-5p, Let-7b-3p, miR-24-3p, miR-361-5p, miR-335-5p, miR-337-3p, miR-134-5p. Real-time PCR was performed using the miRCURY LNA miR PCR Assay and normalized to *U6* RNA and relative to WAT. Differentially expressed miR (fold change ≥ 0.5) are indicated in yellow, which represents upregulated miRNA in BAT compared to WAT, and in blue are the downregulated miRs (fold change ≤ -0.5) in BAT compared to WAT. $N = 3/\text{group}$. **(b)** RT-PCR analysis of transcript abundance of BAT thermogenic and mitochondrial markers *Ucp1*, *Cs*, and *Cris1* in BAT compared to WAT. mRNA expression values were normalized to *L7* mRNA. $N = 8/\text{group}$. **(c)** RT-PCR analysis of mmu-miR-337-3p expression in mouse WAT and BAT normalized to *U6* RNA. $N = 8/\text{group}$ **(d)** RT-PCR analysis of mmu-miR-337-3p abundance in BAT, WAT, liver, kidney, small intestine, skeletal muscle, pancreas, brains, and lungs presented as percentage of mmu-miR-337-3p transcript abundance from its expression in BAT. Expression of miR-337-3p in BAT is set to 100%. **(e)** Representative image of the genomic mapping of miR-337-3p in humans and conservation of its seed sequence among species. Data are presented as means \pm SEM; individual data points are given by the dot plot. Either Mann–Whitney-U or Independent sample *t*-test was used to assess differences in expression levels. ### $p < 0.001$ Mann–Whitney-U, ** $p < 0.01$ **** $p < 0.0001$ Independent sample *t*-test, equal variances not assumed. n, number of biological replicas; WAT, white adipose tissue; BAT, brown adipose tissue; *Ucp1*, uncoupling protein-1; *Cris1*, cardiolipin synthase 1; *Cs*, Citrate synthase; RT-PCR, quantitative real time-polymerase chain reaction.

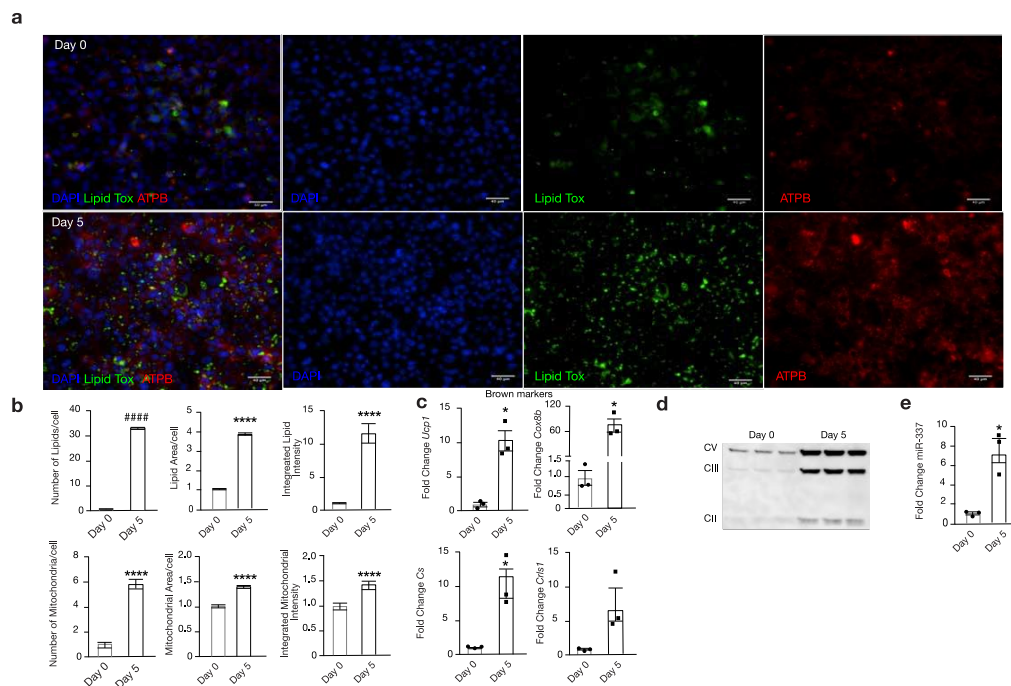


Figure 2. miR-337-3p is upregulated in browning. (a) Representative microscopic images of immunofluorescent stainings from day 0 and day 5 of mouse brown adipocyte differentiation for mitochondria (red) ATPB, lipid droplets (green) Lipidtox, and nuclear (blue) DAPI. The scale bar in the figures corresponds to 40 μ m. (b) Quantifications of number, integrated intensity, and area of mitochondria and lipids corrected per cell of day 0 and day 5 of mouse brown adipocyte differentiation. (n = 6 per group) (c) RT-PCR analysis of BAT thermogenic and mitochondrial markers, *Ucp1*, *Cox8b*, *Cs*, and *Cr1s1* of day 0 and day 5 of mouse brown adipocyte differentiation. L7 mRNA was used as an internal normalizer to the number of mRNA transcript copies. n = 3 per group. (d) Western blot analysis of Complex V (ATP5A-55kDa), III (UQCRC2-48 kDa), and II (SDHB-30kDa) of the electron transport chain of OXPHOS in day 0 and day 5 of mouse brown adipocyte differentiation. (e) RT-PCR analysis of mmu-miR-337-3p in day 0 and day 5 of mouse brown adipocyte differentiation, normalized to U6 RNA. N = 3/group. All immunofluorescent quantifications are presented as medians \pm SD, while quantifications of RT-PCR analysis are presented as means \pm SEM, and individual data points are given by the dot plot. An Independent sample *t*-test was used to assess differences in expression levels. * $p < 0.05$; **** $p < 0.0001$ by Independent sample *t*-test, equal variances not assumed. ##### $p < 0.0001$ Independent sample *t*-test equal variances assumed. n, number of biological replicas; ATPB, β -subunit of ATP synthase; *Ucp1*, uncoupling protein-1; OXPHOS, oxidative phosphorylation; *Cox8b*, cytochrome C oxidase subunit 8b; *Cs*, citrate synthase; *Cr1s1*, cardiolipin synthase 1.

3.3. miR-337 Targets *Twist1*, a Negative Feedback Regulator of Brown Fat Metabolism

Twist1, a class I basic helix–loop–helix transcription factor and negative feedback regulator of *PPARGC1A*/*PPARD*-mediated brown fat metabolism, was identified as a propitious target for modulating brown fat metabolism. We hypothesized that miR-337-3p targets *Twist1* and thereby, prevents the inhibition of brown fat metabolism (Figure 3a) [16]. Indeed, we found *TWIST1* protein abundance to be significantly increased in murine WAT compared to BAT by Western blot analysis, and the inverse of the expression pattern of miR-337-3p (Figures 1c and 3b–c). In line, the seed sequence of miR-337-3p shows perfect complementarity with *Twist1*-3'UTR and is evolutionarily conserved (Figure 3a). The expression of OXPHOS Complex III and Complex IV and UCP1 were increased in BAT compared to WAT, which is inverse to *TWIST1* protein abundance (Figure 3c–e).

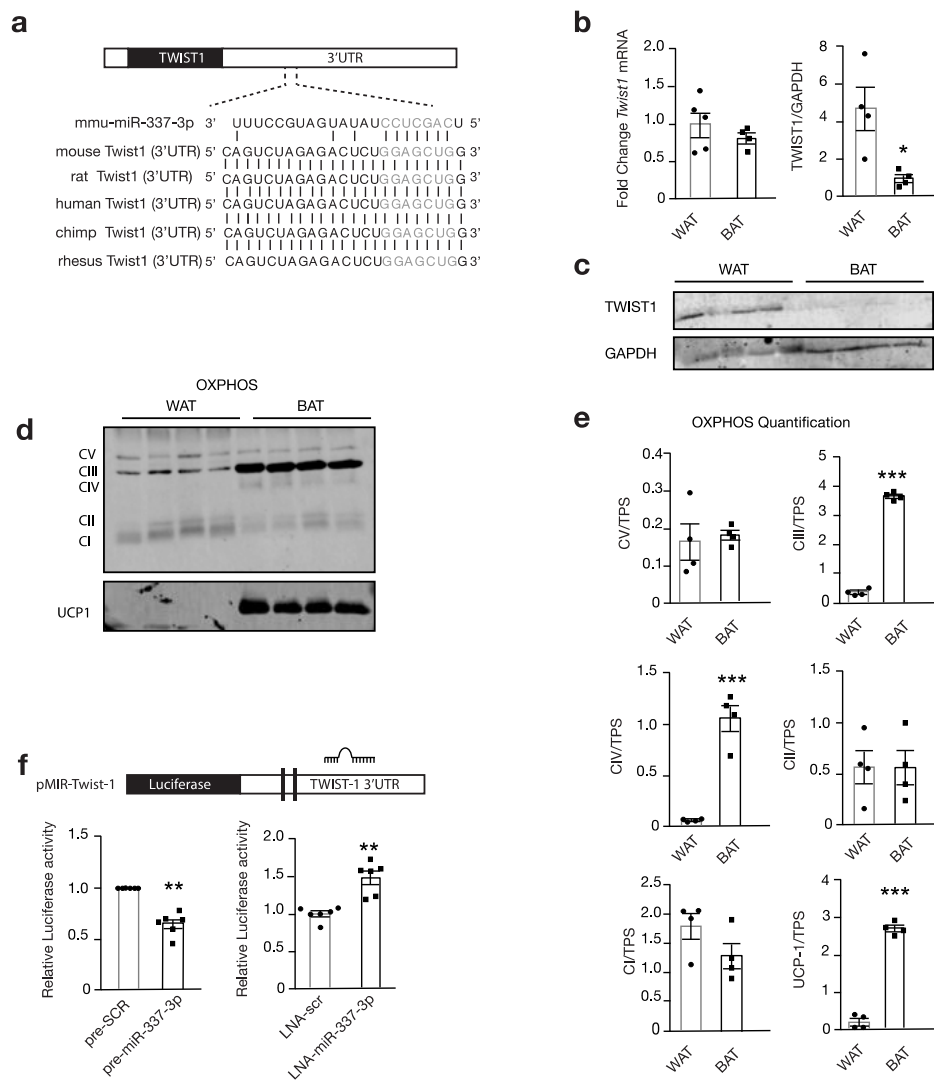


Figure 3. miR-337-3p targets *Twist1*. (a) Schematic representation of predicted seed complementarity between the seed sequence of mmu-miR-337-3p, and seed region on *Twist1* 3'UTR and the evolutionary conservation of this region among species. (b) RT-PCR and Western blot analysis of *Twist1* mRNA expression normalized to 5S (WAT n = 5, BAT n = 4) and TWIST1 protein abundance (WAT n = 4, and BAT n = 5) in mouse WAT and BAT normalized to GAPDH. (c) Representative Western blot of TWIST1 and GAPDH housekeeping protein in mouse WAT and BAT quantified in (b). (d) Western blot of mitochondrial OXPHOS, Complex V, IV, III, II, and I and thermogenic UCP1 protein. (e) Quantification of (d) OXPHOS and UCP1 protein abundance in mouse WAT and BAT normalized to TPS as the loading control. (f) Schematic of luciferase reporter plasmid containing *Twist1* 3'UTR with a binding site for miR-337-3p. Relative luciferase activity quantification in Cos7 cells containing reporter plasmids, co-transfected with either mmu-miR-337-3p precursor or scrambled precursor, and co-transfected with LNA inhibitor for miR-337-3p or LNA inhibitor negative control. Data are presented as means \pm SEM, and individual data points are given by the dot plot * $p < 0.05$; ** $p < 0.01$, by Independent sample *t*-test, equal variances not assumed. *** $p < 0.001$, by Independent sample *t*-test, equal variances assumed. n, number of biological replicas; 3'UTR, 3' untranslated region; OXPHOS, oxidative phosphorylation; UCP1, uncoupling protein-1; GAPDH, Glyceraldehyde 3-phosphate dehydrogenase; *Twist1*, twist-related protein; RT-PCR, quantitative real-time polymerase chain reaction; TPS, total protein stain.

To confirm a physical interaction between miR-337-3p and the *Twist1*-3'UTR, luciferase reporters containing the responsive elements in the 3'UTR of *Twist1* with the hypothesized seed sequence were designed (Figure 3f). Co-transfection of reporter plasmids with precursor molecules for miR-337-3p in COS7 cells decreased luciferase reporter activity compared to transfection with the scrambled precursor, validating a physical interaction causing disruption of luciferase activity. Conversely, co-transfection with the miR inhibitor caused an increased luciferase activity compared to the scrambled inhibitor (Figure 3f). These findings indicate that miR-337-3p targets *Twist1* by interacting with its 3' UTR.

3.4. Modulation of miR-337 Influences *Twist1* and Modulates Mitochondrial Activity and Brown Fat Metabolism

Next, the expression of downstream targets of brown fat metabolism was investigated. Immortalized brown pre-adipocytes reversely transfected with precursor miR-337-3p (Figure 4a) showed a decrease in TWIST1 protein abundance compared to those transfected with the scrambled control (Figure 4b), which paralleled a significantly increased expression of the downstream effector thermogenic uncoupling protein 1, UCP1 (Figure 4c–e). Transfection with miR-337-3p inhibitor showed a significant reduction in UCP1 (Figure 4c–e). Moreover, there was a decreased protein abundance of the OXPHOS Complex V following modulation with miR-337-3p inhibitor (Figure 4d). Taken together, these findings demonstrate that the mitochondrial respiration is increased and favours thermogenesis, as evidenced by an increase in the uncoupling protein inducing brown fat metabolism.

3.5. miR-337/*Twist1* Axis in Metabolic Syndrome Humans

To assess whether the TWIST1-miR-337 axis is functional in humans, we assessed miR-337 and TWIST1 gene expression levels in two forms of WAT: SAT and VAT, from subjects with or without MetS (Figure 5a–c). Correspondingly, we observed a significant increase in miR-337 expression in VAT inverse to the expression of TWIST1 in VAT compared to SAT among MetS subjects (Figure 5a,b). Beside this, expression of miR-337-3p was generally increased in VAT compared to SAT, while expression of TWIST1 was decreased in VAT compared to SAT irrespective of the presence or absence of MetS. Among non-MetS subjects, there was an increased expression of mitochondrial markers, such as *CRLS1* and *CS*, in VAT compared to SAT, whereas the opposite was observed among obese MetS individuals. Mitochondrial oxidative capacity of VAT from MetS subjects was significantly reduced by a decreased expression of *CS* and *CRLS1* compared to non-MetS VAT (Figure 5c). Moreover, the VAT in MetS individuals showed a stronger WAT profile by the expression of *TCF21*, a typical marker of WAT. Taken together, we found a positive correlation between miR-337-3p expression in human adipose tissue and serum high density lipoprotein (HDL) cholesterol levels ($r = 0.715$ $p = 0.013$).

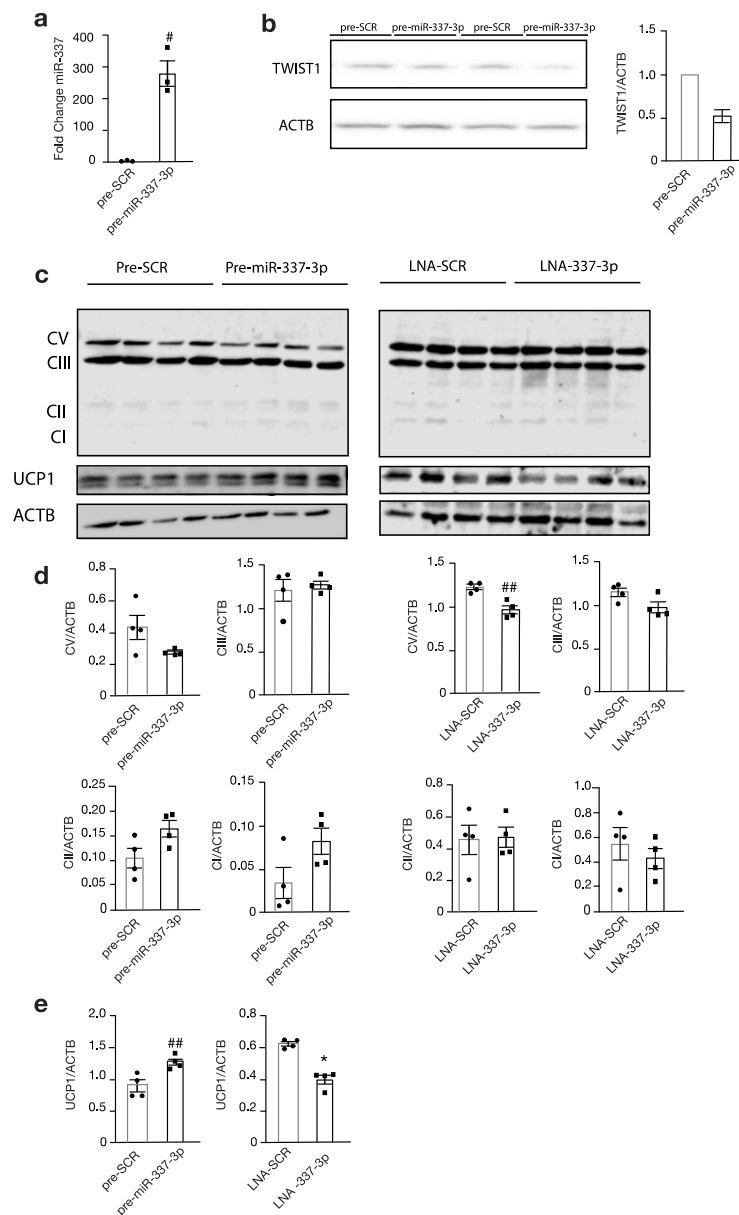


Figure 4. Modulation of miR-337-3p influences Twist1 and downstream thermogenic proteins. (a) RT-PCR analysis of mmu-miR-337-3p in murine brown adipocytes transfected with either precursor mmu-miR-337-3p or precursor scrambled molecule. (b) Western blot analysis of Twist-1 protein abundance of precursor mmu-miR-337-3p or precursor-scrambled transfected brown adipocytes and its quantification on the right (n = 2). (c) Western blot analysis of OXPHOS, Complex V-I, UCP1, and ACTB in brown adipocytes transfected with (left panel) either precursor mmu-miR-337-3p or precursor scrambled, or (right panel) transfected with LNA mmu-miR-337-3p inhibitor or scrambled inhibitor (n = 4 per group). (d) Quantification of OXPHOS Complex V-I protein abundance from (c) Western blot (e) Quantification of UCP1 protein abundance from (c) Western blot. Data are presented as means ± SEM, and individual data points are given by the dot plot. # $p < 0.05$, Independent sample t -test, equal variances not assumed * $p < 0.05$ Mann-Whitney-U for independent samples. ## $p < 0.01$, Independent sample t -test with equality of variances. n, number of biological replicas; OXPHOS, oxidative phosphorylation; UCP1, uncoupling protein 1; ACTB, beta-actin RT-PCR, quantitative real-time polymerase chain reaction.

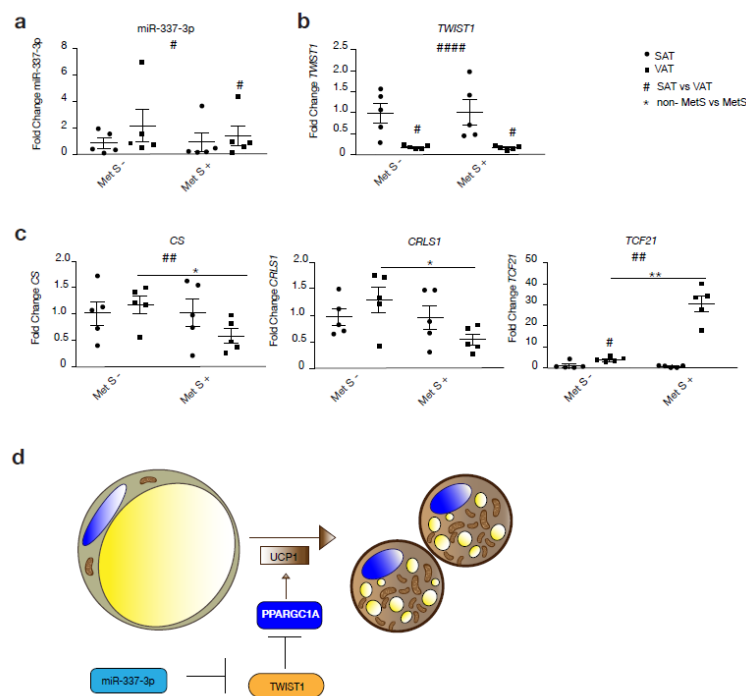


Figure 5. The miR-337-3p and Twist1 axis is disrupted in human subjects with MetS. (a) RT-PCR analysis of hsa-miR-337-3p in human VAT and SAT from non-MetS and MetS human subjects (n = 5/group). (b) RT-PCR analysis of *TWIST1* in human VAT and SAT from non-MetS and MetS human subjects (n = 5 per group). (c) RT-PCR analysis of *TCF21* and mitochondrial genes *CRLS1* and *CS* in VAT and SAT from non-MetS and MetS human subjects (n = 5 per group). (d) Illustration of the pathway proposed in the present study through which miR-337-3p induces browning of adipose tissue. *TWIST1*, when activated, inhibits *PPARGC1A*, which prevents the transcription of genes involved in brown fat metabolism. In summary, miR-337-3p induces translational inhibition of *TWIST1* and prevents transcriptional inhibition of genes involved in the browning of adipose tissue. Data are presented as means \pm SEM, and individual data points are given by the dot plot. *L7* mRNA was used as an internal normalizer to the number of mRNA transcript copies. 5S RNA was used as an internal normalizer to miRNA transcript copies. # $p < 0.05$; ## $p < 0.01$; #### $p < 0.0001$; Paired sample *t*-test (SAT vs. VAT) * $p < 0.05$; ** $p < 0.01$ Independent sample *t*-test (non-MetS vs. MetS), n, number of biological replicas; † VAT, visceral adipose tissue; SAT, subcutaneous adipose tissue; MetS, metabolic syndrome, *TCF21*, transcription factor 21; *CS*, citrate synthase; *CRLS1*, cardiolipin synthase 1; *PPARGC1A*, peroxisome proliferator-activated receptor-gamma coactivator-1 alpha; *UCP1*, uncoupling protein 1.

4. Discussion

The present study demonstrates that miR-337-3p induced repression of *Twist1*, enhancing BAT specific gene expression and protein abundance in brown adipocytes. We demonstrated that miR-337-3p is highly expressed in BAT compared to WAT, and is increased during the differentiation of brown adipocytes. Although no previous associations have been made between miR-337-3p and browning of adipose tissue, a previous study has shown that this miR correlates with protection against saturated fatty acid-induced insulin resistance in mouse muscle cells [18]. Therefore, the described function of miR-337-3p in the present study could be a mediator of the contribution of BAT in glucose homeostasis and regulates insulin sensitivity [19].

We found that miR-337-3p exerts its effect by targeting *Twist1*. In line, the elevated expression of miR-337-3p in BAT compared to WAT was accompanied by a reduced *Twist1* protein abundance in BAT compared to WAT, and was accompanied by increased expression of browning markers. Nairismägi analysed the presence of conserved miR target sites in the 3'UTR of the *Twist1* gene and identified for the first time miR-337-3p in combination with miR-151-5p, and miR-145a-5p and

miR-151-5p as strong regulators of *Twist1* [20]. Heterozygous knockout mice of *Twist1* showed an obesity-resistant phenotype when placed on a high-fat diet and increased brown fat metabolism by elevated oxygen consumption, mitochondrial biogenesis, and uncoupling in BAT [16]. Recent studies have shown that overexpression of *Twist1* is metabolically unfavourable as it indirectly contributes to fat accumulation, while the silencing of *Twist1* enhances insulin sensitivity of adipocytes by antagonizing mitochondrial damage [21]. Moreover, in brown adipocytes, *Twist1* interacts directly with *Ppargc1a* and serves as a key regulator of a negative feedback regulatory loop, orchestrating the balance between *Ppargc1a* induced transcription of target genes involved in uncoupling and *Ppard* isoform controlled brown fat metabolism resulting in a balanced energy homeostasis in response to energy substrate availability [16,22].

We performed a functional analysis that showed that overexpression of miR-337-3p leads to a decrease in TWIST1 and an increase in UCP1 protein abundance. UCP1 is a downstream effector present in the mitochondrial membrane and necessary for the brown fat specific thermogenic function. [23,24]. To confirm that there is an interaction between the miR and the 3'UTR of the target gene, reporter plasmids containing the 3'UTR of *Twist1* were co-transfected with miR-337-3p, which validated the predicted seed complementarity between miR-337-3p and *Twist1*-3'UTR. Previously, Nairismägi et al. reported that miR-337-3p required the presence of miR-151-5p to induce translation inhibition of *Twist1*, although the data were not confirmed by Western blot analysis, but relied solely on luciferase reporter measurements [20]. Besides this, these experiments were performed on H1299 cells, a human non-small cell lung carcinoma cell line, while we performed our experiments in mouse brown adipocytes. In contrast to what this group has shown, in our model reverse transfection with miR-337-3p precursor was enough to induce translational inhibition not only validated by using reporter plasmids but also by direct measurement of TWIST1 protein abundance by Western blot analysis.

To date, obesity has reached large proportions worldwide, causing the development of high mortality comorbidities, such as diabetes, cardiovascular disease, and cancers. This underlines the dire need for novel treatment paradigms. In the present study, the human translatability and the potential for clinical application are substantiated by the validation of the inverse relationship between miR-337-3p and *Twist1* shown in human adipose tissue samples. While miR-337-3p is increased, *Twist1* is decreased in VAT compared with SAT. These findings are accompanied by an increase or a decrease in mitochondrial markers (CRLS1 and CS) in healthy subjects (however, not significant) and MetS obese subjects VAT, respectively. In physiological conditions, one would expect that following an increase in miR-337-3p and a decrease in *Twist1*, an increase in the mitochondrial markers occurs. However, due to pathologic alterations attributed to MetS, the level of mitochondrial markers was decreased instead. The distribution of adipose tissue in obese individuals gives a tremendous amount of information on the cardiometabolic risk profile in humans [25]. In obesity, increased visceral adipose tissue distribution consistently confirms a strong association with metabolic complications and cardiovascular disease and malignancies [25–28]. The “unhealthy” profile of VAT in MetS obese subjects with a reduction in mitochondrial activity is in line with previous studies that reported impaired mitochondria activity in metabolic disorders, such as obesity and metabolic syndrome [29,30]. It seems that the effect of obesity and MetS in VAT is higher than the one produced by the effect by miR-337-3p increased, and *Twist1* decreased. This deficit provides the possibility of a therapeutic window, aiming at counteracting mitochondrial dysfunction in adipose tissue from obese individuals. Although an important limitation of the present study is the small sample size of the human cohort. The results shown here for human data are in accordance with previous findings in literature. Particularly, CRLS1, a primary mediator in the activation and recruitment of thermogenic fat correlates positively with insulin sensitivity and could reduce insulin resistance in MetS [31]. Not only did miR-337-3p seem to have a beneficial effect on the expression of thermoregulatory and mitochondrial genes in adipose tissue, but this miR also correlated positively with serum levels of HDL cholesterol. HDL cholesterol is known for its beneficiary effects in reducing atherosclerotic plaques by reverse cholesterol transport [2]. These findings suggest multiple beneficiary effects possible by miR-337-3p. However, key to accomplishing these beneficiary

effects and prior to clinical translation, future research should be directed towards the development of vehicles that allow delivery of the miR only to adipose tissue, to prevent off-target effects in other tissues that could potentially be harmful.

Conclusively, we here demonstrated that miR-337-3p targets Twist1, which is involved in the suppression of mitochondrial metabolism and function in brown adipocytes. Therefore, modulation of Twist1 by miR-337-3p represents a potential strategy to counteract obesity and its metabolic alterations. To date, previous studies have shown that subcutaneous WAT is able to take on many of the “visceral fat”-like molecular characteristics through miR-mediated signaling [32]. Moreover, human VAT is more prone to adopt a brown fat phenotype upon activation, raising interesting grounds for possible differentiation into mature brown fat [24,33]. Future studies could focus on different strategies for the delivery of this miR specifically to VAT to convert harmful VAT in beneficial energy combustion, to accomplish its beneficial effects.

Supplementary Materials: The following are available online at <http://www.mdpi.com/2073-4409/9/4/1056/s1>, Table S1: Anthropometric and clinical characteristics of healthy and metabolic syndrome subjects: Table S2: Strategy for selecting gene of interest and literature search.

Author Contributions: I.G.C.V. performed experiments, analysed the data, and wrote the manuscript. H.e.A. contributed to the conception and design of the study, analysis and interpretation of data. S.O. performed experiments and analysis of data. A.V. performed experiments and analysis of data J.d.B. supervised the project. P.A.d.C.M. edited the manuscript. F.J.T. provided samples. L.J.d.W. contributed to the conception and design of the study, contributed to discussion, and reviewed/edited manuscript. M.M. contributed to the conception and designed the study, performed experiments, analysis and interpretation of the data, and wrote the manuscript. All authors have read and agreed to the published version of the manuscript.

Funding: P.A.d.C.M. is supported by a MEERVOUD grant from The Netherlands Organisation for Scientific Research and is an Established Investigator of the Dutch Heart Foundation (NHS2015T066). L.J.d.W. acknowledges support from the Netherlands CardioVascular Research Initiative: the Dutch Heart Foundation, Dutch Federation of University Medical Centers, ZonMW, and the Royal Netherlands Academy of Sciences. L.D.W. was further supported by grant 311549 from the European Research Council (ERC) and a VICI award 918-156-47 from NWO. F.J.T. is supported by grant PI18/01160 from the Instituto de Salud Carlos III (ISCIII) co-funded by FEDER funds, and by the CIBER Fisiopatología de la Obesidad y Nutrición (CIBEROBN) of the Institute of Health Carlos III (ISCIII) (CB06/03/0018), Spain. M.M. is supported by Miguel Servet I program (CP17/00133) from ISCIII and co-funded by FEDER funds. M.M. is also supported by UMA18-FEDERJA-285 co-funded by Malaga University, Junta de Andalucía, and FEDER funds, CB06/03/0018 and PI-0297-2018 co-funded by FEDER funds and Consejería de Salud y Familia, Junta de Andalucía, Spain.

Acknowledgments: We thank Bruce Spiegelman (Harvard University) for the kind gift of the immortalized mouse brown adipocyte cell line.

Conflicts of Interest: The authors declare no conflict of interest, except P.A.d.C.M. and L.J.d.W. who are co-founders and stockholders of Mirabilis Therapeutics BV.

Abbreviations

ACTB	(actin beta)
ATP	(adenosine triphosphate)
ATPB	(β -subunit of ATP synthase)
BAT	(brown adipose tissue)
Crls1	(cardiolipin synthase 1)
Cs	(Citrate synthase)
GAPDH	(glyceraldehyde- 3 Phosphate dehydrogenase)
miR	(micro-RNA)
MetS	(Metabolic syndrome)
OXPHOS	(oxidative phosphorylation)
PPARGCIA	(peroxisome proliferative activated receptor, gamma, co-activator alpha)
PPARD	(peroxisome proliferative activated receptor delta)
RT-PCR	(real-time polymerase chain reaction)
SAT	(subcutaneous adipose tissue)
TPS	(total protein stain)
Twist1	(twist family basic helix–loop–helix transcription factor 1)
CP1	(uncoupling protein1)
3'UTR	(3' untranslated region)
VAT	(visceral adipose tissue)
WAT	(white adipose tissue)

References

1. Ng, M.; Fleming, T.; Robinson, M.; Thomson, B.; Graetz, N.; Margono, C.; Mullany, E.C.; Biryukov, S.; Abbafati, C. Global, regional, and national prevalence of overweight and obesity in children and adults during 1980–2013: A systematic analysis for the Global Burden of Disease Study 2013. *Lancet* **2014**, *384*, 766–781. [[CrossRef](#)]
2. Huang, P.L. A comprehensive definition for metabolic syndrome. *Dis. Model. Mech.* **2009**, *2*, 231–237. [[CrossRef](#)] [[PubMed](#)]
3. Deepa, M.; Papita, M.; Nazir, A.; Anjana, R.M.; Ali, M.K.; Narayan, K.M.; Mohan, V. Lean people with dysglycemia have a worse metabolic profile than centrally obese people without dysglycemia. *Diabetes Technol. Ther.* **2014**, *16*, 91–96. [[CrossRef](#)] [[PubMed](#)]
4. Goossens, G.H.; Blaak, E.E. Adipose tissue dysfunction and impaired metabolic health in human obesity: A matter of oxygen. *Front. Endocrinol.* **2015**, *6*, 55. [[CrossRef](#)]
5. Sanchez, J.C.; Converset, V.; Nolan, A.; Schmid, G.; Wang, S.; Heller, M.; Sennitt, M.V.; Hochstrasser, D.F.; Cawthorne, M.A. Effect of rosiglitazone on the differential expression of obesity and insulin resistance associated proteins in lep/lep mice. *Proteomics* **2003**, *3*, 1500–1520. [[CrossRef](#)]
6. Enerback, S. Human brown adipose tissue. *Cell Metab.* **2010**, *11*, 248–252. [[CrossRef](#)]
7. Wu, J.; Bostrom, P.; Sparks, L.M.; Ye, L.; Choi, J.H.; Giang, A.H.; Khandekar, M.; Virtanen, K.A.; Nuutila, P.; Schaart, G.; et al. Beige adipocytes are a distinct type of thermogenic fat cell in mouse and human. *Cell* **2012**, *150*, 366–376. [[CrossRef](#)]
8. Shimizu, I.; Aprahamian, T.; Kikuchi, R.; Shimizu, A.; Papanicolaou, K.N.; MacLauchlan, S.; Maruyama, S.; Walsh, K. Vascular rarefaction mediates whitening of brown fat in obesity. *J. Clin. Investig.* **2014**, *124*, 2099–2112. [[CrossRef](#)]
9. Kusminski, C.M.; Scherer, P.E. Mitochondrial dysfunction in white adipose tissue. *Trends Endocrinol. Metab.* **2012**, *23*, 435–443. [[CrossRef](#)]
10. Li, P.; Jiao, J.; Gao, G.; Prabhakar, B.S. Control of mitochondrial activity by miRNAs. *J. Cell Biochem.* **2012**, *113*, 1104–1110. [[CrossRef](#)]
11. Andreux, P.A.; Houtkooper, R.H.; Auwerx, J. Pharmacological approaches to restore mitochondrial function. *Nat. Rev. Drug Discov.* **2013**, *12*, 465–483. [[CrossRef](#)]
12. Murri, M.; El Azzouzi, H. MicroRNAs as regulators of mitochondrial dysfunction and obesity. *Am. J. Physiol. Heart Circ. Physiol.* **2018**, *315*, H291–H302. [[CrossRef](#)] [[PubMed](#)]
13. Yu, J.; Lv, Y.; Wang, F.; Kong, X.; Di, W.; Liu, J.; Sheng, Y.; Lv, S.; Ding, G. MiR-27b-3p Inhibition Enhances Browning of Epididymal Fat in High-Fat Diet Induced Obese Mice. *Front. Endocrinol. (Lausanne)* **2019**, *10*, 38. [[CrossRef](#)] [[PubMed](#)]
14. Christopher, A.F.; Kaur, R.P.; Kaur, G.; Kaur, A.; Gupta, V.; Bansal, P. MicroRNA therapeutics: Discovering novel targets and developing specific therapy. *Perspect. Clin. Res.* **2016**, *7*, 68–74. [[PubMed](#)]
15. De Majo, F.; De Windt, L.J. RNA therapeutics for heart disease. *Biochem. Pharmacol.* **2018**, *155*, 468–478. [[CrossRef](#)] [[PubMed](#)]
16. Pan, D.; Fujimoto, M.; Lopes, A.; Wang, Y.X. Twist-1 is a PPARdelta-inducible, negative-feedback regulator of PGC-1alpha in brown fat metabolism. *Cell* **2009**, *137*, 73–86. [[CrossRef](#)]
17. Uldry, M.; Yang, W.; St-Pierre, J.; Lin, J.; Seale, P.; Spiegelman, B.M. Complementary action of the PGC-1 coactivators in mitochondrial biogenesis and brown fat differentiation. *Cell Metab.* **2006**, *3*, 333–341. [[CrossRef](#)]
18. Li, Z.Y.; Na, H.M.; Peng, G.; Pu, J.; Liu, P. Alteration of microRNA expression correlates to fatty acid-mediated insulin resistance in mouse myoblasts. *Mol. Biosyst.* **2011**, *7*, 871–877. [[CrossRef](#)]
19. Stanford, K.I.; Middelbeek, R.J.; Townsend, K.L.; An, D.; Nygaard, E.B.; Hitchcox, K.M.; Markan, K.R.; Nakano, K.; Hirshman, M.F.; Tseng, Y.H.; et al. Brown adipose tissue regulates glucose homeostasis and insulin sensitivity. *J. Clin. Investig.* **2013**, *123*, 215–223. [[CrossRef](#)]
20. Nairismägi, M.L.; Füchtbauer, A.; Labouriau, R.; Bramsen, J.B.; Füchtbauer, E.M. The proto-oncogene TWIST1 is regulated by microRNAs. *PLoS ONE* **2013**, *8*, e66070. [[CrossRef](#)]
21. Lu, S.; Wang, H.; Ren, R.; Shi, X.; Zhang, Y.; Ma, W. Reduced expression of Twist 1 is protective against insulin resistance of adipocytes and involves mitochondrial dysfunction. *Sci. Rep.* **2018**, *8*, 12590. [[CrossRef](#)] [[PubMed](#)]

22. Dobrian, A.D. A tale with a Twist: A developmental gene with potential relevance for metabolic dysfunction and inflammation in adipose tissue. *Front. Endocrinol. (Lausanne)* **2012**, *3*, 108. [[CrossRef](#)] [[PubMed](#)]
23. Cannon, B.; Nedergaard, J. Brown adipose tissue: Function and physiological significance. *Physiol. Rev.* **2004**, *84*, 277–359. [[CrossRef](#)] [[PubMed](#)]
24. Scheele, C.; Nielsen, S. Metabolic regulation and the anti-obesity perspectives of human brown fat. *Redox Biol.* **2017**, *12*, 770–775. [[CrossRef](#)] [[PubMed](#)]
25. Shuster, A.; Patlas, M.; Pinthus, J.H.; Mourtzakis, M. The clinical importance of visceral adiposity: A critical review of methods for visceral adipose tissue analysis. *Br. J. Radiol.* **2012**, *85*, 1–10. [[CrossRef](#)]
26. Sam, S. Differential effect of subcutaneous abdominal and visceral adipose tissue on cardiometabolic risk. *Horm. Mol. Biol. Clin. Investig.* **2018**, *33*. [[CrossRef](#)]
27. Tang, L.; Zhang, F.; Tong, N. The association of visceral adipose tissue and subcutaneous adipose tissue with metabolic risk factors in a large population of Chinese adults. *Clin. Endocrinol. (Oxf.)* **2016**, *85*, 46–53. [[CrossRef](#)]
28. Verboven, K.; Wouters, K.; Gaens, K.; Hansen, D.; Bijnen, M.; Wetzels, S.; Stehouwer, C.D.; Goossens, G.H. Abdominal subcutaneous and visceral adipocyte size, lipolysis and inflammation relate to insulin resistance in male obese humans. *Sci. Rep.* **2018**, *8*, 4677. [[CrossRef](#)]
29. Chan, D.C. Mitochondria: Dynamic organelles in disease, aging, and development. *Cell* **2006**, *125*, 1241–1252. [[CrossRef](#)]
30. Phielix, E.; Mensink, M. Type 2 diabetes mellitus and skeletal muscle metabolic function. *Physiol. Behav.* **2008**, *94*, 252–258. [[CrossRef](#)]
31. Sustarsic, E.G.; Ma, T.; Lynes, M.D.; Larsen, M.; Karavaeva, I.; Havelund, J.F.; Nielsen, C.H.; Jedrychowski, M.P.; Moreno-Torres, M.; Lundh, M.; et al. Cardioprotein Synthesis in Brown and Beige Fat Mitochondria Is Essential for Systemic Energy Homeostasis. *Cell Metab.* **2018**, *28*, 159–174.e11. [[CrossRef](#)] [[PubMed](#)]
32. Ding, H.; Zheng, S.; Garcia-Ruiz, D.; Hou, D.; Wei, Z.; Liao, Z.; Li, L.; Zhang, Y.; Han, X.; Zen, K.; et al. Fasting induces a subcutaneous-to-visceral fat switch mediated by microRNA-149-3p and suppression of PRDM16. *Nat. Commun.* **2016**, *7*, 11533. [[CrossRef](#)] [[PubMed](#)]
33. Yang, X.; Sui, W.; Zhang, M.; Dong, M.; Lim, S.; Seki, T.; Guo, Z.; Fischer, C.; Lu, H. Switching harmful visceral fat to beneficial energy combustion improves metabolic dysfunctions. *JCI Insight* **2017**, *2*, e89044. [[CrossRef](#)] [[PubMed](#)]



© 2020 by the authors. Licensee MDPI, Basel, Switzerland. This article is an open access article distributed under the terms and conditions of the Creative Commons Attribution (CC BY) license (<http://creativecommons.org/licenses/by/4.0/>).